Effect of the Pauli principle on the deformed quasiparticle random-phase approximation calculations and its consequence for β-decay calculations of deformed even-even nuclei

Dong-Liang Fang
College of Physics, Jilin University, Changchun, Jilin 130012, China
(Received 4 December 2015; revised manuscript received 16 January 2016; published 8 March 2016)

In this work, I take into consideration the Pauli exclusion principle (PEP) in the quasiparticle random-phase approximation (QRPA) calculations for the deformed systems by replacing the traditional quasiboson approximation (QBA) with the renormalized one. With this new formalism, the parametrization of QRPA calculations has been changed and the collapse of QRPA solutions could be avoid for realistic g_{pp} values. I further find that the necessity of the renormalization parameter of particle-particle residual interaction g_{pp} in QRPA calculations is due to the exclusion of PEP. So with the inclusion of PEP, I could easily extend the deformed QRPA calculations to the less-explored region where lack of experimental data prevent effective parametrization of g_{pp} for QRPA methods. With this theoretical improvement, I give predictions of weak decay rates for even-even isotopes in the rare-earth region and compare the results with existing calculations.

DOI: 10.1103/PhysRevC.93.034306

I. INTRODUCTION

Rapid neutron-capture process (r-process) plays an important role in the formation of our solar system element abundance and it is thought to be responsible for productions of most heavy elements [1] beyond ^{56}Fe. As a result of interest in the determination of the site for this process, various models have been proposed, i.e., the hot high entropy neutrino wind model [2], the cold neutron star mergers model [3], etc. This process requires large neutron-to-seed-nuclei ratios at the initial phase, while the r-process path and the final abundance are determined by the competitions between the neutron-capture rates and the weak decay rates at the late stage. In this sense, precise values of weak decay rates, especially for isotopes along or around the r-process path, become crucial for the simulation of this process. Unfortunately most of these isotopes are neutron rich and very unstable, which makes most of them out of the reach of current rare-isotope experiments. Thus, one needs to rely on accurate theoretical predictions of these properties in order to understand what is happening during these processes. Efforts have been devoted to this topic over decades, i.e., with the global calculations microscopic or gross [4–6].

Besides these global calculations over the whole nuclide chart, there are also numerous approaches devoted to calculating nuclei in specific regions; e.g., the large-scale shell model (LSSM) calculations have been adopted for calculations for magic or semimagic nuclei [7,8], which are usually with spherical shapes so that spherical symmetry could be imposed. For these nuclei, methods such as spherical QRPA with various kinds [9–11] are also applicable, and their agreement among each other has been improved steadily. Not all the nuclei are in spherical shapes, for open-shell nuclei lie deep in the center of the square area surrounded by the magic lines on the nuclide chart, permanent deformations have been observed, and for these nuclei spherical symmetry is heavily broken. Simulation shows that the r-process path goes through two such deformed regions: The first is the Kr-Mo region (region I hereafter) and another is the neutron-rich rare-earth region (region II). For region I, exotic neutron-rich isotopes far from the stability line have been measured recently (e.g., for Zr isotopes, those with 16 more neutrons than stable ones have been measured); see, for example, Refs. [12,13]. This ease the r-process simulation and could improve our understandings of the shape of $A \sim 140$ peak of the abundance pattern. Theorists have also calculated rates of these nuclei with, for example, the deformed QRPA methods, either self-consistently with the Skyrme [14,15] or Gogny [16] forces or the traditional non-self-consistent case with realistic interactions [17,18]. On the other hand, the situation for region II is less satisfying for these deformed isotopes, because their heavy mass and difficulty of production and storage pose obstacles to measuring their basic properties such as mass or decay rates. Currently only a small number of them have been measured; for example, the heavily deformed Nd isotopes of six neutrons beyond quasistable ^{150}Nd nucleus have been experimentally accessed.

As pointed out in Refs. [19,20], weak decay properties of these nuclei could be crucial for the long-standing problem of element abundance, the rare-earth peak. If we observe the abundance pattern, besides the two giant peaks near A $\sim$ 140 and A $\sim$ 190 caused by two shell gaps around neutron number $N = 82,126$, we could find also a bump (or peak) near $A \sim 165$. The formation of this peak has been investigated in Refs. [19,20] with different mechanisms such as quenched shell gaps or fission back from heavy nuclei. They show that to distinguish from these different mechanisms, we need more accurate nuclear data such as masses or weak decay properties for hundreds of nuclei in the deformed rare-earth region. In the absence of experimental data mentioned above, we resort to theories. Not many calculations have been done for this region compared to region I. There are global calculations from Ref. [6], but no alternatives are available. Reference [21] has provided some of the rates with fitted parameters from well-measured spherical nuclei. In this work, I introduce the renormalized quasiparticle random-phase approximation (rQRPA) methods for the calculations of even-even nuclei by considering the Pauli exclusion principle (PEP) approximately. I find that the deviation of a renormalization parameter of the

realistic particle-particle residual interaction (or the namely the strength of the interaction) g_{pp} from 1 is largely due to the ignorance of the PEP. With approximate treatment of PEP in QRPA approaches by the boson mapping technique, one could use bare G-matrix elements for the realistic nuclear structure calculations, that is, $g_{pp} = 1$. I compare my results to the measurements as well as calculations from Ref. [6]. Decent agreements have been achieved in both regions discussed above. This article is arranged as follows: In Sec. II I give detailed formalisms of the method, then I discuss the parameters in Sec. III, followed by results and discussions in Sec. IV, and finally the conclusion.

II. FORMALISM

For the deformed system, single-particle wave functions are generally described in the intrinsic frame, and they are usually expanded on specific basis [22]:

$$|\Omega_\tau\rangle = \sum_{\{N\}\Lambda\Sigma} b^{\Omega_\tau}_{\{N\}}|\{N\}\Lambda\rangle|\Sigma\rangle. \tag{1}$$

Here $\{N\}$ is a set of quanta, i.e., with the deformed harmonic oscillator (HO) basis, there are $\{n_z,n_\rho\}$. Here, Λ is projection of orbital angular momentum on symmetry axis z of the axially deformed system, and Σ are the projection of spin on this axis.

The QRPA method is based on quasiparticle representation, which is derived by solving either the BCS or Hatree-Fock Bogoliubov (HFB) equations. In my calculations, I use the BCS method to treat the nuclear pairing, and under this scenario, the quasiparticle operators can be expressed as

$$\alpha_\tau = u_\tau c^\dagger_\tau + v_\tau \tilde{c}_\tau. \tag{2}$$

Here u's and v's are the so-called BCS coefficients.

I then define the proton-neutron QRPA (pn-QRPA) phonon for the charge-exchanging case as

$$\begin{aligned} Q^{m\dagger}_{K^\pi} &= \sum_{pn} X^m_{pn} A^\dagger_{pn} - Y^m_{pn}\tilde{A}_{pn}, \\ \Omega_p + \Omega_n &= K. \end{aligned} \tag{3}$$

In order to get these forward- and backward-amplitude X's and Y's, I then use the variational methods as explained in Refs. [23,24] to derive the so-called pn-QRPA equations [25,26]. Here the two-quasiparticle creation operator is defined as $A_{pn} = \alpha^\dagger_p\alpha^\dagger_n$.

The commutation relations $[A_{pn},A^\dagger_{p'n'}] = \delta_{pp'}\delta_{nn'}$ are usually used in the derivation of these QRPA equations; this is the so-called quasiboson approximation (QBA), which treats the combination of two quasiparticle creation operators as a boson operator. However, this commutation relation is not exact since it neglects the Pauli exclusion principle (PEP) for a multifermion system. In this work, I go beyond this approximation by replacing this commutation relation with the one used previously in Refs. [27–29] for spherical systems:

$$\begin{aligned} [A_{pn},A^\dagger_{p'n'}] &= \delta_{pp'}\delta_{nn'} - \delta_{pp'}\langle 0^+_{QRPA}|\alpha^\dagger_{n'}\alpha_n|0^+_{QRPA}\rangle \\ &\quad - \delta_{nn'}\langle 0^+_{QRPA}|\alpha^\dagger_{p'}\alpha_p|0^+_{QRPA}\rangle \\ &= \mathcal{D}_{pp',nn'}. \end{aligned} \tag{4}$$

This is the so-called renormalized quasiboson approximation (rQBA). A general assumption here is that under QRPA vacuum, only diagonal terms exist, and this implies that only nucleon pairs with $K^\pi = 0^+$ contribute to the coefficients $\mathcal{D}$. By applying this new commutation relation, I could obtain the QRPA equations in the form

$$\begin{pmatrix} \mathcal{A} & \mathcal{B} \\ -\mathcal{B}^* & -\mathcal{A}^* \end{pmatrix}\begin{pmatrix} X \\ Y \end{pmatrix} = \omega\mathcal{D}\begin{pmatrix} X \\ Y \end{pmatrix}. \tag{5}$$

Here the QRPA matrices are defined as in Refs. [25,26]: $\mathcal{A}_{pn,p'n'} = [A_{pn},(H,A^\dagger_{p'n'})]$ and $\mathcal{B}_{pn,p'n'} = [\tilde{A}_{pn},(H,\tilde{A}_{p'n'})]$.

For the convenience of calculations, I follow the notations introduced in Ref. [29]: $\bar{A}(\bar{B}) = \mathcal{D}^{-1/2}\mathcal{A}(\mathcal{B})\mathcal{D}^{-1/2}$ and $\bar{X}(\bar{Y}) = \mathcal{D}^{1/2}X(Y)$. With this convention, the QRPA equation now has the form

$$\begin{pmatrix} \bar{A} & \bar{B} \\ -\bar{B}^* & -\bar{A}^* \end{pmatrix}\begin{pmatrix} \bar{X} \\ \bar{Y} \end{pmatrix} = \omega\begin{pmatrix} \bar{X} \\ \bar{Y} \end{pmatrix}. \tag{6}$$

The new forms of the QRPA equations are the same as the old ones with X and Y now replaced by $\bar{X}$ and $\bar{Y}$, so the same technique of solving the QRPA equations could be applied here. The $\mathcal{D}$'s could be obtained approximately with the boson-mapping methods introduced in Ref. [27]:

$$\begin{aligned} B^\dagger_{pp'} &\to \sum_n B^\dagger_{pn}B_{p'n}, \\ B^\dagger_{nn'} &\to \sum_p B^\dagger_{pn}B_{pn'}, \end{aligned}$$

where B is defined as $B^\dagger_{\tau\tau'} = \alpha^\dagger_\tau\alpha_{\tau'}$. There is an exact derivation of $\mathcal{D}$ with a solvable model [30], which implies that my treatment could have deviations with large particle-particle interaction strength from the exact solutions; this will be discussed later. With this boson-mapping approach, I get the expression for $\mathcal{D}$ as

$$\begin{aligned} \mathcal{D}_{pnp'n'} = \delta_{pp'}\delta_{nn'}\Bigg(1 &- \sum_{p''} D_{p''np''n'}\sum_m \bar{Y}^m_{p''n}\bar{Y}^m_{p''n'} \\ &- \sum_{n''} D_{pn''p'n''}\sum_m \bar{Y}^m_{pn''}\bar{Y}^m_{p'n''}\Bigg). \end{aligned} \tag{7}$$

Equations (7) and (6) could be solved iteratively to give the final solutions of the renormalized QRPA (rQRPA) equations.

The expression of β-decay matrix elements is now a bit different; for the allowed β-decay matrix elements, I have in the intrinsic system the expression

$$\begin{aligned} M_{GT}(E_i) &= \langle K,i|\tau^-\sigma^1_K|0^+\rangle \\ &= \sum_{pn}\langle p|\sigma_K|n\rangle\mathcal{D}^{1/2}_{pn}\left(u_pv_n\bar{X}^i_{pn} + v_pu_n\bar{Y}^i_{pn}\right). \end{aligned} \tag{8}$$

Here $K = 0,\pm1$ and $E_i = \omega^K_i - \omega_{lst}$ follows the definition in Ref. [17] with ω_{lst} the lowest eigenvalues from QRPA equations of all K^π. The single-particle matrix elements $\langle p|\sigma|n\rangle$ are expressed in Refs. [17,26]. The first forbidden (FF) matrix elements are in similar style but with much more complicated expressions [17]. The details of the calculations of half-lives in the deformed systems with these calculated

matrix elements are also presented in Ref. [17],;I will not give the details here.

III. PARAMETERS

For the mean field, I use the same wave functions as in Ref. [17] obtained by solving the Schrödinger equation with Woods-Saxon potentials parametrized as in Refs. [17,31]. For the sake of comparison in region II with other results, in this work, for the choice of deformation parameters, if they are available from the measured data [32], I use the experimental values; otherwise I adopt the predicted values from finite range droplet model (FRDM) [33] instead of those from HFB17 [34] used in Ref. [17]. The same strategy is used for the parametrization of nuclear masses—I use the values from FRDM model [33] unless they are experimentally available [32]; with these masses, I could then get the β-decay Q values (the errors from measurements will be considered, as I will show later) as well as pairing gaps from the five-point formula [36]. By adjusting the pairing strength parameters d_{pp} and d_{nn}, which are overall renormalization factors for the realistic G-matrix elements, I fit these calculated pairing gaps. These choices of parameters deviated from those in Ref. [17], which will also lead to deviation of the final decay rates from those in Ref. [17], as shown in Fig. 2.

For the residual interaction, as in Ref. [17], I use the G matrix with realistic charge dependent-Bonn potential. The two most important parameters in my approach are the renormalization strength of residual interactions in the particle-hole channel (g_{ph}) and particle-particle channel (g_{pp}). The former is related to the position of GTR and does not affect the low-lying structure for this parameter, so I use the value as explained in Ref. [17]. (This is also partially because rQBA does not affect particle-hole interactions.) The latter parameter g_{pp} is crucial for β-decay half-lives; I present my strategy for this parameter in detail later. Before discussing this, I first concentrate on another parameter g_A in the nuclear system. As it is known that the measured Gamow-Teller (GT) strength amounts only about 60% to the model-independent Ikeda sum rule from various experiments, this raises a problem about the quenching of the axial vector constant g_A. I will not go into details about the origin of this quenching, but simply use the value $g_A = 0.75 g_{A0}$ extracted from various experiments such as Ref. [35]. It is known that rQRPA would violate the Ikeda sum rule [29], but my calculation shows that this suppression of GT strength affects more of the resonance than the low-lying part. Hence for β decay, which is related to the low-lying part of GT strength, a quenching factor the same as that for QRPA could be used.

In this work, as I have mentioned above, I focus on two deformed regions which are on the r-process path. For the Kr-Mo region (region I), β-decay half-lives of most nuclei have been measured recently [12,13], while for the important rare-earth region (region II), at present, most neutron-rich nuclei are still out of the reach of the experimental facilities; nevertheless, there are urgent needs for accurate predictions of their weak decay properties as these are important inputs for r-process abundance simulations with extra importance on the formation of the so-called rare-earth peak [19,20]. In this work I adopt

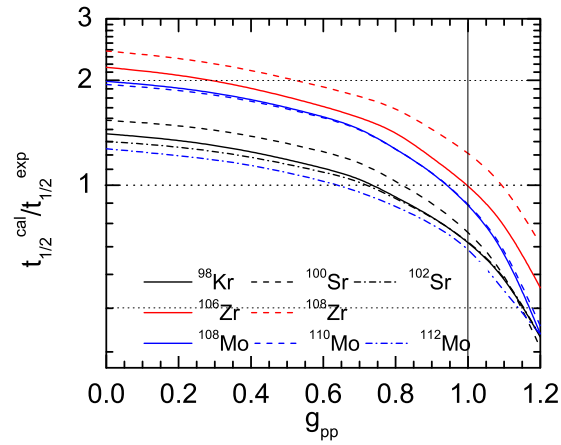

FIG. 1. Illustration of half-life dependence on particle-particle residual interaction strength g_{pp} from rQRPA calculation with realistic forces.

model space larger than that used [17] ($N = 0$–6 vs $N = 0$–5) for region I, and for region II, an even larger model space of $N = 0$–7 is used to eliminate possible errors from model space truncation. My calculation show that enlargement of the model space in region I causes just a small change of about several percent for decay rates; this is small relative to the errors of the many-body model—QRPA itself. The reason is that most low-lying GT or first forbbiden (FF) transitions occurs between levels near Fermi surface, and contributions from levels far below or far above Fermi energy are relatively small, especially for low-lying states. In Ref. [17], I have found sensitive dependence of the half-lives on the particle-particle strength g_{pp}, which calls for accurate determination of this parameter as mentioned above. In this work, I follow the treatment in Ref. [17] by finding proper value of g_{pp} from the dependence of $t_{1/2}$ on g_{pp}, as is illustrated in Fig. 1. If I compare the current $t_{1/2}^{\text{theo.}}/t_{1/2}^{\text{exp.}} - g_{pp}$ curves with those in Fig. 2 of [17] I will find that the curves have been stretched out at the x direction, which is caused by the relaxation of overcorrelation of residual interactions in the particle-particle channel with the inclusion of PEP. The values of g_{pp} in QRPA calculations are possibly affected be several factors such as the model space or PEP. In this work, the model space issue has been carefully handled by using a pretty large model space. With this treatment, my arguments are now that the major reason for the necessity of g_{pp} in QRPA calculations is than the overcorrelation from PEP violation. So in this sense, when PEP effects have been considered, I could use bare G-matrix elements of realistic forces in QRPA calculations, and the main errors produced by this treatment are from the approximation of my boson mapping method instead of exact realization of PEP. The advantage of this treatment is now straightforward, that I could handle the regions where fitting of the parameter g_{pp} are nearly impossible due to the lack of experimental data. To see the validity of the above arguments, we could check the errors in Fig. 1 when the bare G matrix is used in particle-particle channel, namely, $g_{pp} = 1$. Following the vertical lines in the figure, we see that the calculated half-lives deviate the experimental ones by at most 30% and the

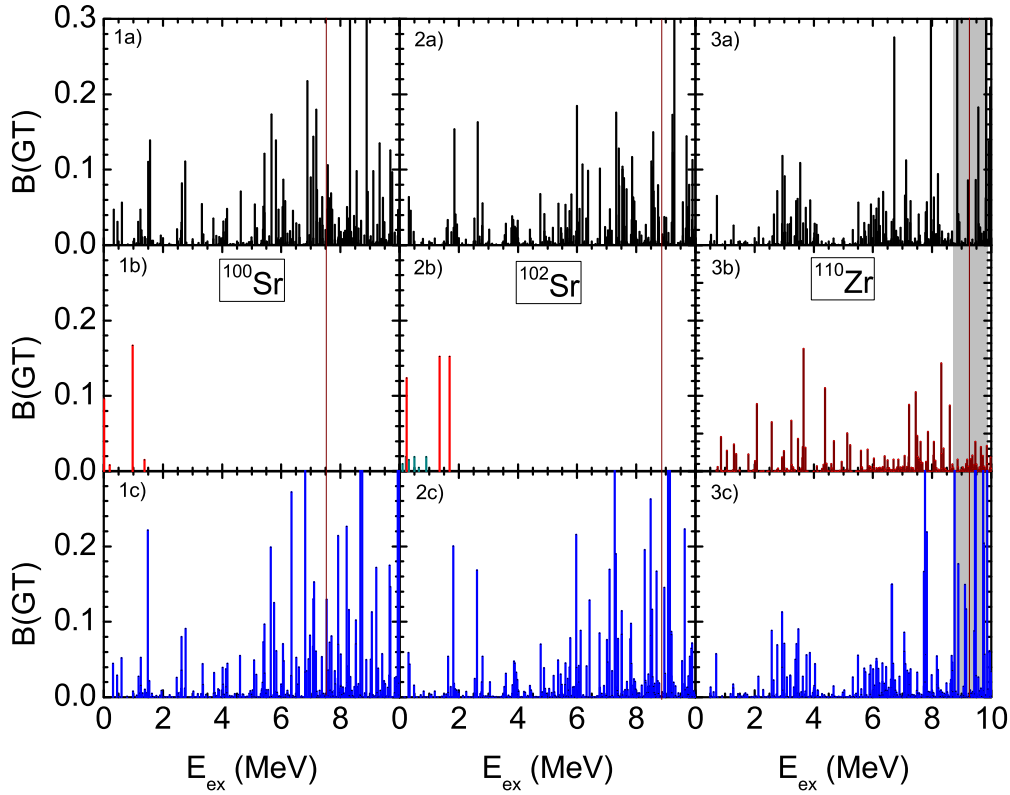

FIG. 2. The *B(GT)* strength distributions for three nuclei, ^{100}Sr, ^{102}Sr, and ^{110}Zr. The black droplines are results from QRPA calculations (panels marked with a) and blue lines for rQRPA calculations (marked with c). (1b) and (2b) are experimental strengths extracted from Ref. [32], where red lines are GT transitions and green lines are probably GT transitions. (3b) is taken from Ref. [17] from QRPA calculations with parameters different from current calculation. The vertical lines are the Q values, for ^{110}Zr, and the shaded area denotes the uncertainty of the Q value.

general trend is that the theory slightly overpredicted the decay rates. The reason for this is that residual interaction in the particle-particle channel is still a bit overcorrelated with boson mapping approximation from conclusions in Ref. [30], where they have compared the exact treatment and boson mapping technique with a solvable model. With this in mind, I could draw a conclusion that violation of PEP is the main source of a heavy renormalization of residual interaction in previous QRPA calculation. I will check the validity of this conclusion further with more nuclei in both regions and give predictions of the weak decay properties for more even-even isotopes in the next section.

IV. RESULTS AND DISCUSSION

As I have shown above, the renormalization parameter g_{pp} introduced in previous QRPA calculations is somehow due to the violation of PEP with large model space. This would lead to the conclusion that for rQRPA with a large model space, using a bare G matrix in the particle-particle channel could be an optimal choice. To see the robustness of this conclusion, I make comparisons between theoretical calculations and experimental results for more isotopes. First I concentrate on region I, where there has been recently evaluated data [12] as well as older data [13]. The recent data improve the accuracy for many isotopes in this region; for most nuclei the measured half-lives are the same and the deviations of the recent data from the older data are small. Reference [13] also presents more decay rates for nuclei with more neutrons. The results of QRPA calculations taken from Ref. [17] are compared to QRPA calculation with the same formalism but with different parameters of masses and deformations, as well as the improved results from rQRPA; this arrangement is to separate the changes due to PEP from those caused by modifications of parameters. For rQRPA calculations, I also introduce the errors of Q values with newest evaluations from the NNDC database [32], and the Q values have change a bit since Ref. [17], where they were taken from Ref. [36]. This causes deviations for some nuclei. For masses those are experimentally unavailable, I use values from Ref. [33], as mentioned above. The recent parameters of masses and deformations cause changes to my final results, especially the mass parameters, as they are related to the pairing parameters Δ and β-decay Q values. The effect of another parameter—the deformation on QRPA calculations—is discussed in Ref. [14]. Deviations of about a factor of two for theories are encountered for some nuclei, but for those less neutron-rich, the rates basically stay the same. This can easily be interpreted from less modification of mass parameters for these nuclei. Well-fitted $g_{pp} = 0.75$ values in Ref. [17] basically reproduce the experimental results for even-even nuclei, as we see from Fig. 1 of [17]. The comparison between

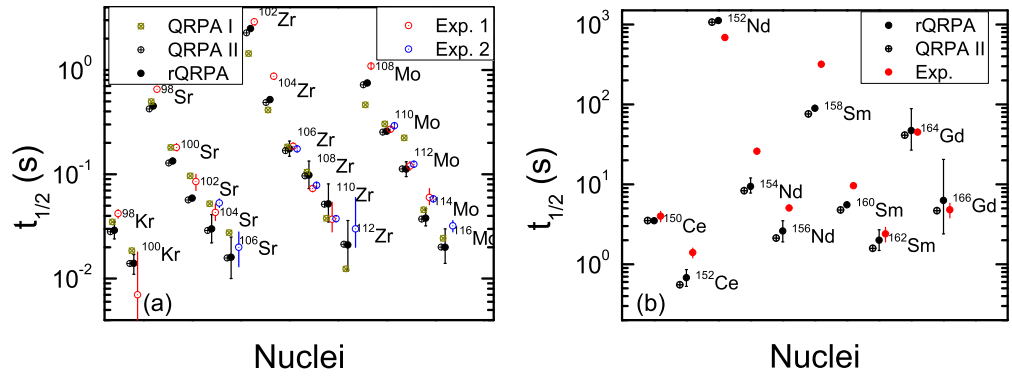

FIG. 3. Comparison of results among calculated and measured half-lives of even-even isotopes in the Kr-Mo region (left panel) and rare-earth region (right panel). For left panel, QRPA I denotes results from Ref. [17] with QRPA calculations and QRPA II denotes QRPA calculations with the mass and deformation parameters used in this work. rQRPA denotes results with PEP in this work. Exp1 indicates measured rates from Ref. [12] or national nuclear data center (NNDC) if not presented and Ref. [32]; Exp 2 indicates rates from recent measurements in Ref. [13]. For the right panel, the rQRPA denotes results from this work and Exp. denotes results from NNDC [32]. The error bars of my theoretical calculations come from error bars of Q values from NNDC [32].

QRPA and rQRPA results in this work with the same set of parameters consolidates my conclusion in previous section that bare G-matrix elements used in rQRPA are suitable, provided the fact that results using this arrangement agree with QRPA results with previously fitted g_{pp} almost exactly. This, on the other hand, shows that renormalization parameters g_{pp} previously used for realistic forces come mainly from the negligence of PEP in the calculation.

Comparing the calculated results with the measurements, I find that for most nuclei the agreement is satisfying except for a few Sr isotopes. The errors of the calculation are generally within a factor of two and for most isotopes the deviations are even smaller. The uncertainties from current mass measurements produce large errors for the final rates; improvement of mass evaluations or empirical mass assessments are needed to enhance the prediction power of current β-decay theory. Inclusion of more isotopes generally does not change my conclusion drawn for less isotopes in Fig. 1; at this region, the decay half-lives are from seconds to milliseconds and the general errors follow those in Fig. 3 of Ref. [17]. This error is important as most nuclei along the r-process path are with half-lives of this magnitude. It is reasonable to estimate that the general error of QRPA calculations for these r-path nuclei should be of the similar magnitude. This estimation would help determine the uncertainty analysis in r-process simulations such as those done in Ref. [37].

To understand how the inclusion of PEP changes QRPA calculations and the reason for the similarity of QRPA and rQRPA results for decay rates with specifically fitted g_{pp}, I need to compare the detailed β-decay strength distributions. As FF decays are weak in this region [17], I compare only the GT strength. From the plotted graph in Fig. 2, one could find that QRPA with renormalized g_{pp} basically reproduces the β strength of rQRPA at a low-energy region for states with excitation energies below 4 MeV. One-to-one correspondence of the low-lying states has been observed, e.g., the three states below 1 MeV with the same transition structure for ^{100}Sr or the two states with large $B(GT)$ values near 2 MeV for ^{102}Sr, as well as the transition around 1 MeV for ^{110}Zr. This correspondence explains the well-behaved β-decay properties from QRPA calculations when PEP is absent. In the meantime, when one goes to the higher energy region with excitation energies above 4 MeV, the deviation starts to emerge. GT strength has been relocated more at this energy region for Sr isotopes but less for ^{100}Zr when PEP is included. These deviations are not important for the decay rates of the isotopes I presented, since their phase space factor is too small to affect the total decay width. But if the Q values become much larger, then they may play a role when their phase space factors become comparable to those of low-lying strength. In this sense, inclusion of PEP may improve the accuracy of decay properties of much more exotic isotopes. For ^{110}Zr, new and old QRPA calculations are compared, and their difference comes from the different deformation from two models as this is the only difference of parametrization in the two calculations. The relocation of strength from changes of deformation have been discussed also in Ref. [17], Fig. 4, and in Ref. [25] for Skyrme calculations; together with this work, one could come to the conclusion that accurate prediction of deformation is vitally important for QRPA calculations. For the two Sr isotopes, I have detailed decay data available, which helps us understand the difference between theory and experiment. The experimental strength is extracted from their decay scheme, so only low-lying strength can be obtained as the contributions of high-lying states to decay width have been suppressed by their small phase space. For each experimental strength below excitation energies of 2 MeV, I could always find correspondence from QRPA calculations, e.g., peak around 1 MeV for ^{100}Sr and two huge transitions around 2 MeV. Theories generally predict the structure of the GT strength transitions. Deviations between theory and experiments are inevitable as far as I could observe, since QRPA is a rough approximation to the exact solutions of nuclear many-body problems. From these graphs, one would naturally raise the problem of whether the deviations could be reduced by adjusting the values of g_{pp}. I will show the answer is negative; from my calculations, I draw the conclusion that increasing g_{pp} would shift more strength to low-lying

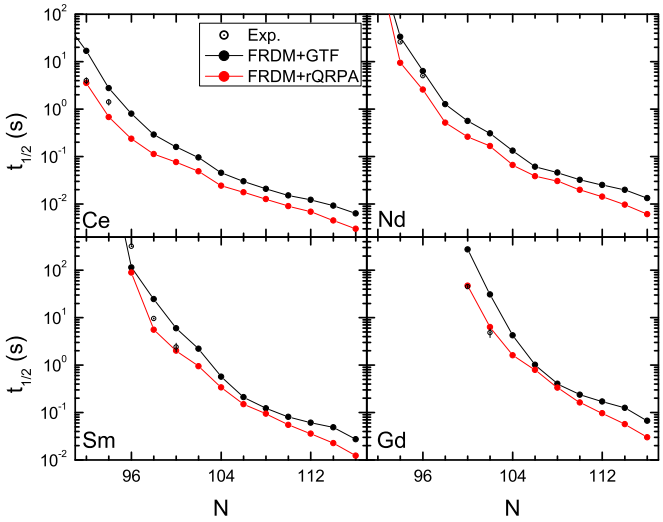

FIG. 4. Prediction of half-lives of even-even nuclei in rare-earth regions from rQRPA calculations. Comparison of my results with decay rates from Ref. [6] and the experiment results [32] are also presented.

states and also 1^+ states to much lower energy, and vice versa. In this sense, if one increases the interaction strength in the pp channel, he could have the 1^+ energies agree with experiments, but the deviations of strength then become much worse. On the other hand, if I reduce the strength g_{pp}, I could have better agreement of strength but worse agreement for excitation energies. So from such analysis, one could see that the deviations between theories and experiments could be related to other issues such as single-particle energies and wave functions or deformation but less from g_{pp}. The possibility of whether the deviation could be reduced by exact treatment of PEP, such as in Ref. [30], still needs investigation.

I now turn my attention to the less-explored region I,I which is also the target of in-constructing facility for rare isotope beam (FRIB); see, e.g., Ref. [38]. This region is not well explored, either theoretically or experimentally, and only a few calculations have been done in this region especially for the neutron-rich isotopes, such as results from Ref. [6] and from Skyrme calculations [21] with tensor forces. Relatively small errors have been achieved from their calculations. In Fig. 3, my attempts are also presented. I also compared the rQRPA results with QRPA results, but now for QRPA, different values of $g_{pp} = 0.63$ are used. These two sets of results agree with each other as in region I. These different values of g_{pp} tell us that without rQRPA, the fitting of g_{pp} is needed; this is usually difficult for deformed regions lack of experimental data. All the known half-lives of those isotopes in this heavily deformed region are longer than 1 s, and these isotopes have much smaller Q values compared with region I, discussed above. Since QRPA values are usually with an error about several hundred keV up to MeV for the prediction of excitation energies, the calculated half-lives could be less accurate compared to those of the previous region where I could have an error of at most a factor of 2 for all isotopes. For these relatively long-lived isotopes, the deviations may be a bit larger than those in region I but still acceptable. It is difficult to claim that my rates are much more precise than other methods with such limited data. In Fig. 3, I have comparisons for several isotopes between my calculations and experiments, and the difference is not so drastic; a factor of two deviation can be obtained for most nuclei except two long-lived isotopes ^{154}Nd and ^{158}Sm. As compared to FRDM rates from Fig. 4, I see better agreements for most Sm and Gd isotopes but they have better predictions for Nd isotopes and similar errors for Ce isotopes. My rates are faster and theirs are slower. Also large errors are encountered in my calculation with the uncertainties from mass measurements, which makes comparison of the results less clear and affects an effective estimation over the errors and reliability of the theory. The errors could be further reduced with the reduction of uncertainties in nuclear mass data, which could be done after FRIB [38].

My results are served as alternatives for the nuclear input of r-process simulations. I did calculations for more nuclei and make comparisons with existing results. The results in Ref. [6] have been widely used in astrophysics community and a direct comparison with them could give us some hints over the final simulation. A large deviation of the two calculations has been observed, and my rates are much faster than theirs. The reason was explained in Ref. [17]: The absence of interactions in particle-particle channel gives overestimation on the half-lives with FRDM model. A factor of two differences between theories have been observed for almost all nuclei here. The consequence of these rates on r-process simulations still needs investigation while rates of all kinds of nuclei can be obtained. This requires extending my formalism to odd-A and odd-odd nuclei with improved accuracies, as previous agreement for these odd nuclei from QRPA calculations in Ref. [17] is really poor. After these have been done, I could make an estimation on how the rates affect the abundance pattern and shed light on the formation of the rare-earth peak.

V. CONCLUSION

In this work I have introduced the rQBA into the QRPA calculations with realistic forces. I found that with the new commutation relation, the over-correlation of residual interactions at pp channel is eliminated, and hence the need of renormalization of these interaction strength can be neglected. With the new calculation, I come to satisfying agreement between calculation and measurement for both regions I and II for neutron-rich even-even isotopes. I also give predictions of half-lives of much neutron-richer nuclei in the rare-earth region, which are important according to simulations from Refs. [19,20]. These calculations would help solve the problem of the formation of the rare-earth peak of the solar element abundance.

ACKNOWLEDGMENTS

I thank B. A. Brown for helpful discussions and comments and J. Engle and T. Shafer for useful discussions on this topic and hospitality during my visit to UNC–Chapel Hill. Correspondence with M. Mumpower is also acknowledged. This work is supported by National Natural Science Foundation of China under Grant No. 11505078.

[1] M. E. Burbidge, G. R. Burbidge, W. A. Fowler, and F. Hoyle, Rev. Mod. Phys. **29**, 547 (1957).

[2] A. Arcones, H. T. Janka, and L. Scheck, Astron. Astrophys. **467**, 1227 (2007).

[3] C. Freiburghaus, S. Rosswog, and F.-K. Thielemann, Astrophys. J. Lett. **525**, L121 (1999).

[4] P. Moller and J. Randrup, Nucl. Phys. A **514**, 1 (1990).

[5] P. Moller, J. R. Nix, and K. L. Kratz, At. Data Nucl. Data Tables **66**, 131 (1996).

[6] P. Moller, B. Pfeiffer, and K. L. Kratz, Phys. Rev. C **67**, 055802 (2003).

[7] T. Suzuki, T. Yoshida, T. Kajino, and T. Otsuka, Phys. Rev. C **85**, 015802 (2012).

[8] Q. Zhi, E. Caurier, J. J. Cuenca-Garcia, K. Langanke, G. Martinez-Pinedo and K. Sieja, Phys. Rev. C **87**, 025803 (2013).

[9] I. N. Borzov, Phys. Rev. C **67**, 025802 (2003).

[10] Z. M. Niu, Y. F. Niu, H. Z. Liang, W. H. Long, T. Niksic, D. Vretenar, and J. Meng, Phys. Lett. B **723**, 172 (2013).

[11] T. Marketin, D. Vretenar, and P. Ring, Phys. Rev. C **75**, 024304 (2007).

[12] S. Nishimura, Z. Li, H. Watanabe, K. Yoshinaga, T. Sumikama, T. Tachibana, K. Yamaguchi, M. Kurata-Nishimura, G. Lorusso, Y. Miyashita, A. Odahara, H. Baba, J. S. Berryman, N. Blasi, A. Bracco, F. Camera, J. Chiba, P. Doornenbal, S. Go, T. Hashimoto, S. Hayakawa, C. Hinke, E. Ideguchi, T. Isobe, Y. Ito, D. G. Jenkins, Y. Kawada, N. Kobayashi, Y. Kondo, R. Krucken, S. Kubono, T. Nakano, H. J. Ong, S. Ota, Z. Podolyak, H. Sakurai, H. Scheit, K. Steiger, D. Steppenbeck, K. Sugimoto, S. Takano, A. Takashima, K. Tajiri, T. Teranishi, Y. Wakabayashi, P. M. Walker, O. Wieland, and H. Yamaguchi, Phys. Rev. Lett. **106**, 052502 (2011).

[13] G. Lorusso *et al.*, Phys. Rev. Lett. **114**, 192501 (2015).

[14] P. Sarriguren and J. Pereira, Phys. Rev. C **81**, 064314 (2010); P. Sarriguren, A. Algora, and J. Pereira, *ibid.* **89**, 034311 (2014); P. Sarriguren, *ibid.* **91**, 044304 (2015).

[15] K. Yoshida, Prog. Theor. Exp. Phys. **2013**, 113D02 (2013).

[16] M. Martini, S. Peru, and S. Goriely, Phys. Rev. C **89**, 044306 (2014).

[17] D. L. Fang, B. A. Brown, and T. Suzuki, Phys. Rev. C **88**, 024314 (2013).

[18] D. Ni and Z. Ren, Phys. Rev. C **89**, 064320 (2014); J. Phys. G. **41**, 125102 (2014).

[19] M. R. Mumpower, G. C. McLaughlin, and R. Surman, Phys. Rev. C **85**, 045801 (2012).

[20] M. Mumpower, G. McLaughlin, and R. Surman, Astrophys. J. **752**, 117 (2012).

[21] M. T. Mustonen, T. Shafer, Z. Zenginerler, and J. Engel, Phys. Rev. C **90**, 024308 (2014).

[22] J. Damgaard, H. C. Pauli, V. V. Pashkevich, and V. M. Strutinski, Nucl. Phys. A **135**, 432 (1969).

[23] P. Ring and P. Schuck, *The Nuclear Many-Body Problem* (Springer Verlag, New York, 1980).

[24] J. A. Halbleib and R. A. Sorensen, Nucl. Phys. A **98**, 542 (1967).

[25] F. Simkovic, L. Pacearescu, and A. Faessler, Nucl. Phys. A **733**, 321 (2004); R. Alvarez-Rodriguez, P. Sarriguren, E. Moya de Guerra, L. Pacearescu, A. Faessler, and F. Simkovic, Phys. Rev. C **70**, 064309 (2004).

[26] M. S. Yousef, V. Rodin, A. Faessler, and F. Simkovic, Phys. Rev. C **79**, 014314 (2009).

[27] F. Catara, N. D. Dang, and M. Sambataro, Nucl. Phys. A **579**, 1 (1994).

[28] J. Toivanen and J. Suhonen, Phys. Rev. Lett. **75**, 410 (1995).

[29] J. Schwieger, F. Simkovic, and A. Faessler, Nucl. Phys. A **600**, 179 (1996).

[30] J. Engel, S. Pittel, M. Stoitsov, P. S. M. Vogel, and J. Dukelsky, Phys. Rev. C **55**, 1781 (1997).

[31] R. Nojarov, Z. Bochnacki, and A. Faessler, Z. Phys. A **324**, 289 (1986).

[32] National Nuclear Data Center, information extracted from the chart of nuclides database, http://www.nndc.bnl.gov/chart/.

[33] P. Moller, J. R. Nix, W. D. Myers, and W. J. Swiatecki, At. Data Nucl. Data Tables **59**, 185 (1995).

[34] S. Goriely, N. Chamel, and J. M. Pearson, Phys. Rev. Lett. **102**, 152503 (2009).

[35] C. J. Guess, T. Adachi, H. Akimune, A. Algora, S. M. Austin, D. Bazin, B. A. Brown, C. Caesar, J. M. Deaven, H. Ejiri, E. Estevez, D. Fang, A. Faessler, D. Frekers, H. Fujita, Y. Fujita, M. Fujiwara, G. F. Grinyer, M. N. Harakeh, K. Hatanaka, C. Herlitzius, K. Hirota, G. W. Hitt, D. Ishikawa, H. Matsubara, R. Meharchand, F. Molina, H. Okamura, H. J. Ong, G. Perdikakis, V. Rodin, B. Rubio, Y. Shimbara, G. Susoy, T. Suzuki, A. Tamii, J. H. Thies, C. Tur, N. Verhanovitz, M. Yosoi, J. Yurkon, R. G. T. Zegers, and J. Zenihiro, Phys. Rev. C **83**, 064318 (2011).

[36] G. Audi, O. Bersillon, J. Blachot, and A. H. Wapstra, Nucl. Phys. A **729**, 3 (2003).

[37] M. Mumpower, R. Surman, D. L. Fang, M. Beard, and A. Aprahamian, J. Phys. G **42**, 034027 (2015); M. R. Mumpower, R. Surman, D.-L. Fang, M. Beard, P. Möller, T. Kawano, and A. Aprahamian, Phys. Rev. C **92**, 035807 (2015).

[38] C. Wrede, EPJ Web Conf. **93**, 07001 (2015).